STARK-MIXING EFFECT ON THE $6p^3\ ^2P_{3/2}$–$6p^3\ ^4S_{3/2}$ TRANSITION IN Bi I

J. KWELA

Institute of Experimental Physics, University of Gdańsk
Wita Stwosza 57, 80-952 Gdańsk, Poland

(Received December 1, 1997; revised version April 21, 1998)

The 301.5 nm electric-field-induced quench radiation on a thermal beam of neutral Bi atoms in the metastable $6p^3\ ^2P_{3/2}$ state for transition to the ground $6p^3\ ^4S_{3/2}$ state was observed. The measurement of the Stark-enhanced intensity of the radiation as a function of the electric field yields a relationship between the field-free-decay rates for transitions between the metastable $6p^3\ ^2P_{3/2}$ state and the nearby states that are mixed in by the field. Using the known decay rates, the measurement sets an approximate transition rate of $A(6p^3\ ^2P_{3/2} \rightarrow 6p^2 7s\ ^4P_{1/2}) \approx (0.50 \pm 0.05)\ \mathrm{s}^{-1}$.

PACS numbers: 32.70.–n, 32.60.+i

1. Introduction

In a series of papers [1–4] we described a technique for determining extremely small decay rates by monitoring the Stark enhancement in the intensity of the radiation emitted by a thermal beam of metastable atoms in the presence of a static electric field.

When the atomic system is placed in an external electric field, states of opposite parity mix. It results in a destruction of the inversion symmetry and a weakening of the parity selection rule. The electric-field perturbation gives rise to a small E1 transition amplitude, as well as M1 and E2 transition amplitudes which normally appear only between states of the same parity. In the experiment reported here, an enhancement in the intensity of the radiation by an electric-field-induced E1 admixture in the $6p^3\ ^2P_{3/2} \rightarrow 6p^3\ ^4S_{3/2}$ (301.5 nm) line of Bi I was observed.

2. Theoretical

The Stark-mixing effect can be described by a first-order perturbation calculus. The external field mixes all even states with the $6p^3\ ^2P_{3/2}$ state, but the most significant contribution comes from the nearby $6p^2 7s\ ^4P_{1/2}$ state from which it is separated by only 576.67 cm^{-1} (see Fig. 1)

$$\left|^2P_{3/2}, M\right\rangle^{\mathrm{E}} = \left|^2P_{3/2}, M\right\rangle + \sum_{M''} \frac{\left\langle ^4P_{1/2}, M''\right| e\boldsymbol{E}\cdot r \left|^2P_{3/2}, M\right\rangle}{E\left(^2P_{3/2}\right) - E\left(^4P_{1/2}\right)} \left|^4P_{1/2}, M''\right\rangle . \quad (1)$$

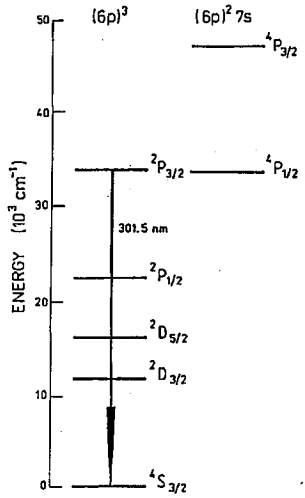

Fig. 1. Energy level diagram for the lower states in Bi I, with the observed mixed (M1 + E2) transition shown.

In the calculations we neglect mixing between the $6p^3\ {}^2P_{3/2}$ and other states of opposite parity because of their large energy separations and for the same reason the perturbation of the ground $6p^3\ {}^4S_{3/2}$ state is ignored.

The probability amplitude of the $6p^3\ {}^2P_{3/2} \rightarrow 6p^3\ {}^4S_{3/2}$ transition in the presence of an external static electric field is proportional to

$$
\begin{aligned}
{}^{\mathrm{E}}\langle {}^2P_{3/2}, M | H^{\mathrm{int}} | {}^4S_{3/2}, M' \rangle^{\mathrm{E}} \propto & -\mathrm{i} \langle {}^2P_{3/2}, M | \boldsymbol{\mu} \cdot \left(\hat{\boldsymbol{k}} \times \hat{\boldsymbol{e}}^* \right) | {}^4S_{3/2}, M' \rangle \\
& + \frac{\omega}{2c} \langle {}^2P_{3/2}, M | \hat{e}^* Q \hat{k} | {}^4S_{3/2}, M' \rangle \\
& + \mathrm{i}\eta \sum_{M''} \langle {}^2P_{3/2}, M | \hat{e} \cdot \boldsymbol{d} | {}^4P_{1/2}, M'' \rangle \langle {}^4P_{1/2}, M'' | eEz | {}^4S_{3/2}, M' \rangle . \qquad (2)
\end{aligned}
$$

Here $\eta^{-1} = E\left({}^2P_{3/2}\right) - E\left({}^4P_{1/2}\right)$, $\boldsymbol{\mu} = \mu_{\mathrm{B}} (\boldsymbol{L} + 2\boldsymbol{S})$, $\boldsymbol{d} = e\boldsymbol{r}$, Q is a dyadic product $Q = e\boldsymbol{r} \otimes \boldsymbol{r}$, and $\hat{\boldsymbol{e}}$ and $\hat{\boldsymbol{k}}$ are unit vectors for the polarization and propagation directions of the emitted photon.

The square of amplitude (2), after averaging over M, summing over M' and polarization directions yields the probability of the ${}^2P_{3/2} - {}^4S_{3/2}$ transition in the presence of the electric field

$$
\begin{aligned}
\sum_{MM'} \left| {}^{\mathrm{E}}\langle {}^2P_{3/2}, M | H^{\mathrm{int}} | {}^4S_{3/2}, M' \rangle^{\mathrm{E}} \right|^2 \propto & \, S_{\mathrm{M1}}\left({}^2P_{3/2}, {}^4S_{3/2}\right) \\
& + \frac{k^2}{20} S_{\mathrm{E2}}\left({}^2P_{3/2}, {}^4S_{3/2}\right) + \frac{1}{6}\eta^2 E^2 S_{\mathrm{E1}}\left({}^2P_{3/2}, {}^4P_{1/2}\right) S_{\mathrm{E1}}\left({}^4P_{1/2}, {}^4S_{3/2}\right) . \qquad (3)
\end{aligned}
$$

Here $k = \omega/c$ and

$$
S_{\mathrm{M1}}(a,b) = |\langle a \| \mu_1 \| b \rangle|^2 , \quad S_{\mathrm{E2}}(a,b) = |\langle a \| Q_2 \| b \rangle|^2 , \quad S_{\mathrm{E1}}(a,b) = |\langle a \| d_1 \| b \rangle|^2 .
$$

It should be noted that the third, field dependent term in (3) gives an isotropic and unpolarized contribution to the intensity. However, when the small additional contributions to the intensity that result from the mixing of the $6p^3\ {}^2P_{3/2}$ state with higher lying even states (hitherto ignored) are taken into account, the sum of all the electric-field-induced E1 terms is slightly anisotropic (see [5]).

We now define the relative enhancement in the intensity of the radiation by the electric field as

$$R = (I^{\mathrm{E}} - I^0)/I^0, \tag{4}$$

where the superscripts refer to the intensities in the presence and absence of the field. Substitution of (3) into this definition yields

$$R = \frac{1}{6}\eta^2\beta E^2, \tag{5}$$

where

$$\beta = \frac{S_{\mathrm{E1}}\left({}^2P_{3/2},\ {}^4P_{1/2}\right) S_{\mathrm{E1}}\left({}^4P_{1/2},{}^4S_{3/2}\right)}{S_{\mathrm{M1}}\left({}^2P_{3/2},\ {}^4S_{3/2}\right) + \frac{k^2}{20} S_{\mathrm{E2}}\left({}^2P_{3/2},\ {}^4S_{3/2}\right)}. \tag{6}$$

3. Experimental

The apparatus used in the experiment is similar to that used previously in the Stark-mixing experiment with the beam of lead [4].

Briefly, bismuth vapor is obtained from a heated oven. The metastable atoms are created by a 1.5 A electrical discharge in the region between the exit nozzle of the oven and a heated tungsten filament. The discharge potential can be set to any desired value in the studied range 2–60 V, by varying the filament temperature. Higher temperatures are required for discharge at lower potentials.

Next the beam passes through a set of collimating slits and after removal of charged particles by a transverse electric field between the deflection plates enters the observation region. Here the 301.5 nm radiation from decay of the metastable atoms in the beam, in the absence and in the presence of a strong electric field, 40–90 kV/cm, is monitored by a photomultiplier (PM) tube (Hamamatsu, model R943-02). The interference filter (Esco Products, Oak Ridge, N.J.) placed in front of the PM has a maximum transmission of 25% at 298 nm and a half bandwidth of 9 nm. The distance of 11 cm from the excitation region to the center of the observation region corresponds to sufficiently long times of flight that all excited states, with the exception of metastable states, will virtually have decayed before they come in view of the solid angle of the detector.

Light intensities are determined by measuring the PM output current with a picoammeter. The PM is cooled to $-100°$C in order to minimize the dark current (0.2×10^{-10} A) at the operating potential of 1900 V. The electric field-free signal-to-noise ratio was improved by a factor of three by mounting the filament directly into the path of the atomic beam in the region between the nozzle of the oven and the entrance slit of the collimator. It was caused by increase in the concentration of the metastable atoms in the beam. This improvement occurred in spite of the fact that the "yellow hot" filament directly underneath the collimator slits introduces a large noise current (1×10^{-10} A) from its black body radiation that can now enter the PM via multiple wall scattering.

The ultimate signal-to-noise ratio achieved was six. Here we define the noise as the signal still observed with the discharge extinguished (by setting the discharge current zero), but with no changes in either the filament or the oven temperature.

4. Observation and results

Once the discharge had been established, relatively stable beams of Bi atoms could be obtained but only for discharge potentials in the range 4–30 V. This allowed the determination of average signal currents, by averaging the PM output over long time intervals of 60 s duration. At a given discharge voltage first the field free signal I^0 and then the signal I^E in the presence of a pre-selected electric field was measured. After correction for background noise, the *relative* enhancement $R = (I^E - I^0)/I^0$ in the intensity was determined at a few field values.

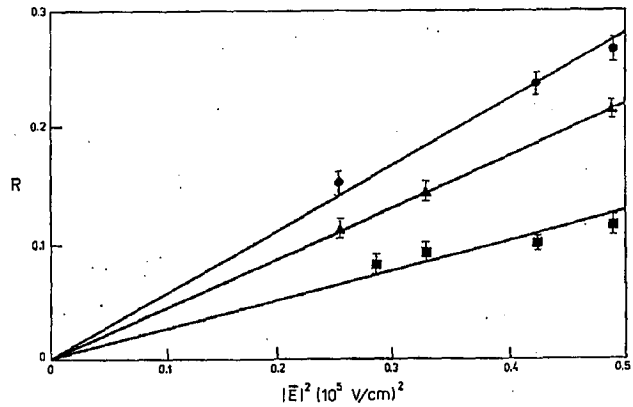

Fig. 2. The field dependence of the Stark-enhanced intensity of radiation for discharge potentials of 4.1 V (o), 13.5 V (△), and 27.5 V (□).

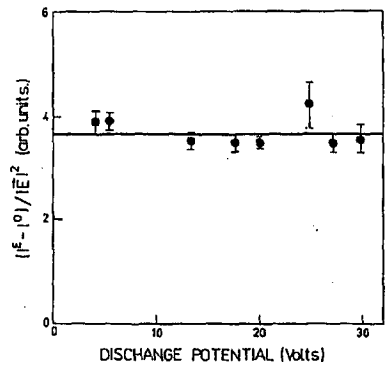

Fig. 3. The Stark-enhanced intensity of radiation, normalized to the square of the electric field, as a function of discharge potential.

Some typical results of the field dependence of R for three discharge potentials of 4.1, 13.5, and 27.5 V are shown in Fig. 2. Each point represents the average of a few measurements and size of the error bar only reflects the fluctuation about the mean. The range of field values is rather limited because the enhancement became too small for reliable measurements at fields below 40 kV/cm, and electrical breakdown between the field plates above 90 kV/cm sets the upper limit.

As expected (see Eq. (5)), it can be seen that R depends quadratically on the electric field, but opposite to the experiment with Pb atoms [4], we obtained different slopes of $R(E^2)$ lines for different discharge voltages. The *absolute* enhancement (I^{E} -- I^0), however, is within experimental error independent of discharge potential, as illustrated in Fig. 3, where the observed absolute enhancements were divided by the square of the electric fields, to which they are proportional.

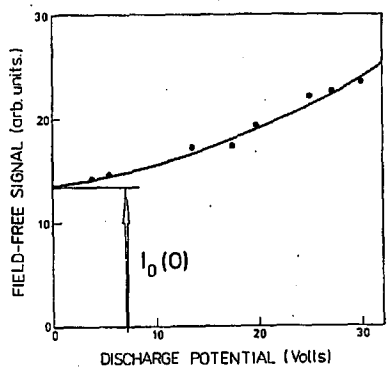

Fig. 4. The dependence of field-free signal on discharge voltage.

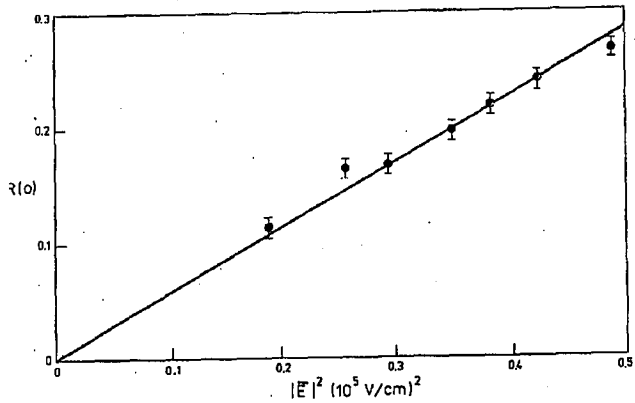

Fig. 5. The electric field dependence of the Stark-enhanced intensity of radiation.

The result of Fig. 3 implies that we can account for the strong voltage dependence of R in Fig. 2 by assuming that only the field free signal, I^0, is affected. Its voltage dependence is shown in Fig. 4, where the solid curve is a best fit of the form

$$I^0(V) = I^0(0) + c_1 V + c_2 V^2, \tag{7}$$

where V is the discharge potential. The form of the polynomial is not crucial for the analysis of the experiment; only the value of $I^0(V)$ extrapolated to zero discharge potential is important. The origin of the voltage dependent part of the radiation is not understood, but it presumably arises from cascade transitions that repopulate the upper energy level of the transition of interest.

We now redefine the relative field enhancement as $R(0) = (I^E - I^0)/I^0(0)$ where $I^0(0)$ is the extrapolated field-free signal. The electric field dependence of $R(0)$ is shown in Fig. 5. Here each point is the average of all our measurements for eight different discharge voltages in the range 4–30 V. That all these points fit within experimental error on a single line, in contrast to the data displayed in Fig. 2, verifies that our data analysis is correct.

5. Analysis

The observed slope $R(0)/E^2 = (5.737 \pm 0.0086) \times 10^{-11}$ (cm/V)^2 for the best fit to the data in Fig. 5 corresponds to $\beta = (6.284 \pm 0.097) \times 10^4\ e^2 a_0^2$. The error in the latter contains the statistical error for the slope as well as the systematic error of the electric field measurement. With the observed β value, Eq. (6) now allows us to find the $A(^2P_{3/2} \rightarrow {}^4P_{1/2})$ decay rate on using experimental values for the transition rates $A_{M1}(^2P_{3/2} \rightarrow {}^4S_{3/2})$, $A_{E2}(^2P_{3/2} \rightarrow {}^4S_{3/2})$, and $A_{E1}(^4P_{1/2} \rightarrow {}^4S_{3/2})$.

We first evaluate $A_{M1}(^2P_{3/2} \rightarrow {}^4S_{3/2})$ and $A_{E2}(^4P_{3/2} \rightarrow {}^4S_{3/2})$ in a semi-empirical way. The angular-momentum coupling for levels of the $6p^3$ configuration is close to the pure jj limit. The calculation of the M1 matrix element depends on the intermediate coupling coefficients and not on the radial parts of the wave functions. For intermediate coupling coefficients we take the ones from [6] since they yield better agreement with experimental results for energy levels and g factors than earlier calculations. In this manner we find $S_{M1} = 0.03\mu_B^2$ and $A_{M1}(^2P_{3/2}-{}^4S_{3/2}) = 8.90\ s^{-1}$. From a comparison between calculated and observed Landé g-factors we find that the error in S_{M1} cannot exceed 5%.

Next we consider the E2 transition rate, which is proportional to the radial integral of r^2 between single-electron states. It can be deduced in the most precise way from experimental results for M1–E2 interference observed in the Faraday [7] or in the Zeeman [8] effects. For states with hyperfine structure both techniques are more sensitive to the value of the radial integral than the measurements of the total intensities of hyperfine components. Recent measurements concerning the radial integral for the $6p^2$ configuration of Bi are given in Table I. With the semi-empirical value of the radial integral we find the E2 component $A_{E2}(^2P_{3/2}-{}^4S_{3/2}) = 0.04\ s^{-1}$.

The M1 and E2 transition rates are known more reliably than $A_{E1}(^4P_{1/2} \rightarrow {}^4S_{3/2})$. The latter can be deduced from the lifetime of the $^4P_{1/2}$ state

TABLE I

Semiempirical values of the radial integral $s_q = e\int_0^\infty P_{6p}r^2P_{6p}dr$ in ea_0^2 units.

Roberts et al.[a]	8.7 ± 0.3
Czerwinska[b]	8.34 ± 0.83
Czerwinska[c]	8.20 ± 0.32
Czerwinska[d]	8.22 ± 0.26
Weighted mean value used in this work	8.4 ± 0.2

[a] Ref. [7].

[b,c,d]Calculated values, using the data of [8] for the percentage admixtures of E2 radiation in the 459.7, 461.5, and 647.6 nm lines of Bi I, respectively.

TABLE II

Experimental lifetimes (in ns) for the $6p^27s\ ^4P_{1/2}$ level of Bi.

Osherovich and Tezikov [9]	4.3 ± 0.2
Anderson et al. [10]	4.7 ± 0.7
Svanberg [11]	4.75 ± 0.18
Weighted mean value used in this work	4.55 ± 0.13

and from branching ratio measurements. Results for the most accurate lifetime measurements are given in Table II. The experimental value of the $A\left(^4P_{1/2} \rightarrow ^4S_{3/2}\right) / \sum_k A\left(^4P_{1/2} \rightarrow k\right)$ branching ratio is 0.946 which is stated to be reliable to 8% [12]. From this we deduce $A(^4P_{1/2} \rightarrow {}^4S_{3/2}) = (2.08 \pm 0.17) \times 10^8\ \mathrm{s}^{-1}$, which is in agreement with the calculations of [13] and with Ref. [14].

Using the experimental values for the transition rates above we finally obtained that $S_{\mathrm{E1}}(^2P_{3/2} \rightarrow {}^4P_{1/2}) = (5.13 \pm 0.50) \times 10^{-3}\ (ea_0)^2$ corresponding to a transition rate of $A(^2P_{3/2} \rightarrow {}^4P_{1/2}) = (0.50 \pm 0.05)\ \mathrm{s}^{-1}$. Here the greatest part of the error arises from the uncertainty in $A_{\mathrm{E1}}(^4P_{1/2} \rightarrow {}^4S_{3/2})$.

The experimental value of $A(^2P_{3/2} \rightarrow {}^4P_{1/2})$ was determined by limiting our attention to contribution to the Stark-mixing amplitude only from the $6p7s\ ^4P_{1/2}$ state. The obtained result is the first approximate estimate of $A_{\mathrm{E1}}(^2P_{1/2} \rightarrow {}^4P_{1/2})$ in Bi and no theoretical data exists for comparison.

6. Conclusion

The experiment has directly provided a connection between the four decay rates of Eq. (8). Three of these four rates can in principle be measured by standard methods in spectroscopy, but no technique, other than the Stark mixing used in this experiment, exists to measure the transition rate between the very close lying $6p^27s\ ^4P_{1/2}$ and $6p^3\ ^2P_{3/2}$ levels.

The Stark-mixing technique, of course, is rather limited. A numerical value for a transition rate can be arrived at only if the related ones are known. However, even if none of these transition probabilities were known, a relation between them still has merit since it provides a consistency test for future measurements.

This work was supported by the Committee for Scientific Research grant 2 P302 084 07.

References

[1] J. Kwela, *Z. Phys D* **6**, 25 (1987).

[2] J. Kwela, Z. Konefał, R. Drozdowski, J. Heldt, *Z. Phys. D* **9**, 215 (1988).

[3] J. Kwela, A. van Wijngaarden, *Phys. Rev. A* **42**, 6360 (1990).

[4] J. Kwela, *Z. Phys. D* **32**, 35 (1994).

[5] J. Kwela, *Z. Phys. D* **13**, 101 (1989).

[6] D.A. Landman, A. Lurio, *Phys. Rev. A* **1**, 1330 (1970).

[7] G.J. Roberts, P.E.G. Baird, M.W.S.M. Brimicombe, P.G.H. Sanders, D.R. Selby, D.N. Stacey, *J. Phys. B* **13**, 1389 (1980).

[8] J. Czerwińska, *J. Opt. Soc. Am. B* **4**, 1349 (1987).

[9] A.L. Osherovich, V.V. Tezikov, *Opt. Spektrosk. (Russia)* **44**, 219 (1978).

[10] T. Anderson, O.H. Madsen, G. Sorensen, *J. Opt. Soc. Am.* **62**, 1118 (1972).

[11] S. Svanberg, *Phys. Scr.* **5**, 72 (1972).

[12] Y. Guern, J. Lotrian, A. Bideau-Mehu, A. Johannin-Gilles, *J. Phys. B* **11**, 3821 (1978).

[13] L. Holmgren, *Phys. Scr.* **11**, 15 (1975).

[14] V.V. Flambaum, O.P. Sushkov, *J. Quant. Spectrosc. Radiat. Transf.* **20**, 569 (1978).